MAUSAM, **72**, 2 (April 2021), 331-348

551.577.3 : 553.21 (235.512)

Rainfall characteristics and its variability over a high-altitude station in Western Ghats during southwest monsoon of 2015 - A case study

S. G. NARKHEDKAR, S. N. DUTTA*, V. ANILKUMAR, S. MUKHERJEE

and G. PANDITHURAI

Indian Institute of Tropical Meteorology, Pashan, Pune, Maharashtra, India

**India Meteorological Department, MoES, Pune – 411 005, India*

(*Received 31 January 2020, Accepted 27 November 2020*)

e mail : narkhed@tropmet.res.in

सार – भारत में पश्चिमी घाट के पर्वतीय स्थल महाबलेश्वर (MBL) में वर्षा की विशेषताओं (पर्वतीय और संवहनीय) का इस शोध पत्र में अध्ययन किया गया है। पहले भाग में इस केंद्र में वर्षा की मात्रा निर्धारित करने में पर्वतीय और संवहनीय अस्थिरता की भूमिका की जांच की गई है। दूसरे भाग में, MBL में वर्षा की परिवर्तनशीलता का विश्लेषण किया गया है। 3-डी गतिकीय मॉडल का उपयोग करके पर्वतीय वर्षा का अनुमान लगाने के लिए, एक उच्च-विभेदन वाले ईसीएमडब्ल्यूएफ पुनर्विश्लेषण डेटा का उपयोग एक सुदूरवर्ती स्थान में पवन और तापीय क्षेत्रों के निर्माण के लिए किया गया। जबकि, संवहनीय वर्षा का अनुमान लगाने के लिए, ईसीएमडब्ल्यूएफ पुनर्विश्लेषण डेटा और MBL में स्वस्थाने रेडियोसोंडे डेटा का उपयोग किया जाता है। यह देखा गया है कि संवहनीय मॉडल के उपयोग से अनुमानित वर्षा की तुलना में पर्वतीय वर्षा के 3-डी गतिकीय मॉडल के उपयोग से अनुमानित वर्षा, दैनिक प्रेक्षित वर्षा के पैटर्न के अनुरूप है। इसके अलावा, वर्षा के दैनिक उतार-चढ़ाव को अंकित करने में अनुमानित वर्षा सक्षम रही। हालांकि, प्रेक्षित वर्षा की तुलना में संवहनीय मॉडल के उपयोग से पैटर्न और परिमाण में बहुत अंतर देखा गया।

वायुविलय और उनकी विशेषताओं के साथ बड़े पैमाने की सिनॉप्टिक प्रणाली की भी वर्षा परिवर्तनशीलता पर उनके प्रभाव को समझने के लिए जांच की गई। MBL में वायुविलय की परिवर्तनशीलता और प्रेक्षित वर्षा से पता चलता है कि वे विशिष्ट रूप से सहसंबद्ध हैं।

ABSTRACT. The rainfall characteristics (orographic and convective) over Mahabaleshwar (MBL), a Western Ghat hill station in India, has been studied in this work. In the first part, the role of orography and convective instability in quantifying rainfall over the station has been examined. In the second part, the variability of rainfall over MBL has been analyzed. In order to estimate orographic rainfall using a 3-D dynamical model, a high-resolution ECMWF reanalysis data was utilized to construct wind and thermal fields at a far upstream location. Whereas, for estimating convective rainfall, the ECMWF reanalysis data and in situ radiosonde data over MBL are used. It is seen that the estimated rainfall using the 3-D dynamical model for orographic rainfall is in good agreement with the pattern of observed daily rainfall as compared to the estimated rainfall using the convective model. Also, the estimated rainfall was able to capture the daily fluctuations in the rainfall. However, the rainfall estimated using the convective model shows much difference in the pattern and magnitude compared to the observed rainfall.

Large scale synoptic systems along with aerosols and their characteristics were also examined to understand their influence on rainfall variability. The variability of aerosols and the observed rainfall over MBL reveals that they are significantly correlated.

Key words – High altitude station, Orographic rainfall, convective rainfall, 3-D dynamical orographic model, Large scale synoptic systems, Characteristics of aerosols.

1. Introduction

Rainfall distribution at a place is significantly affected by the orographic barrier at that place. Orography at a place enhances rainfall by the forced ascent of moist air and by triggering convection or both of them. Whereas, the convective rainfall occurs due to the thermal convection currents caused by the heating of ground due to solar insolation. The warm air rises and expands and reaches a cooler layer and saturates, resulting in the condensation in the form of cumulus or cumulonimbus clouds. Whereas, the orographic rainfall occurs due to the

ascent of moist air forced by the mountain barrier. The mountain barrier should be across the wind direction so that the moist air is forced in obstruction to move upward and gets cooled and condensed. It is also well known that mountains play an important role in developing deep convection by acting as an elevated heat source. Orography also enhances the convection over high altitude stations.

Earlier studies, *viz*., Sarker (1966, 1967) and De (1973) also suggested that along with forced orographic ascent, synoptic scale convergence and convective instability are important factors for the occurrence of heavy rainfall on the windward slope. Grossman and Duran (1984) studied the influence of the WGs, in the formation of deep convective cells away from the mountain crest on the windward side. Watnabe and Ogura (1987) showed that a mountain range of modest height could trigger the convective instability to enhance rainfall significantly along the windward slope. De and Dutta (2005) studied the convective instability during contrasting rainfall epochs over Mumbai, situated on the west coast at mean sea level. They observed that the coastal station, Mumbai, lying on the windward side of WG, receives heavy rainfall on an isolated day with preceding and succeeding days of comparatively low rainfall or dry weather. In this study a simple convective precipitation model was developed and they showed that estimated rainfall, computed using this model, could well captured, at least qualitatively, the observed day to day fluctuation of rainfall. They further concluded that in such cases, forced orographic lifting alone is not the only mechanism responsible for such observed heavy rainfall. In addition to that, convective instability may also play a crucial role along with synoptic-scale convergence. Therefore, the study of the role of convective instability in enhancing the orographic rainfall rate becomes more important. All these studies highlight the importance of the combined effect of orography and convection on the rainfall over the mountainous region.

On the basis of the above studies and considering the variability in the observed daily rainfall, an attempt has been made to study the rainfall characteristics of MBL. The rainfall is estimated using orographic and convective precipitation models and compared with the observed rainfall. Orographic rainfall and convective precipitation models used in this study have been used successfully by De and Dutta (2005) and Dutta (2007), respectively, over various regions of the Indian subcontinent. Bonacina (1945) surveyed the regions of heavy orographic rain around the world and their possible mechanisms. He concluded that orographic rain does not occur every time an airstream impinges on a mountain; rather, the prevailing synoptic situation must condition air stream. He further emphasized the importance of convective instability for the generation of intense orographic rain. Heavy rainfall events along the west coast stations of India are observed when the monsoon current is strong both in the Arabian Sea and Bay of Bengal under the influence of synoptic systems (Madan *et al*., 2005).

While studying the characteristics of the rainfall over MBL, the possible effect of aerosols on the variability of its rainfall has also been studied. A sub-set of atmospheric aerosol can serve as cloud condensation nuclei (CCN) and a minor fraction could act as an ice nuclei (IN). These particles play a crucial role in controlling the microphysical properties of orographic clouds and potentially affect the orographic precipitation development. An increase in the CCN shifts the cloud droplet size spectrum toward smaller radii and reduces the efficiency of the collision/coalescence processes in warm phase clouds (Twomey *et al*., 1984; Peng *et al.*, 2002; Lowenthal *et al*., 2004; Anil Kumar *et al.*, 2016). The overall implications of the indirect aerosol effect on orographic clouds and precipitation at different spatial and temporal scales are inconclusive and uncertain for both observational and modeling studies (Menon *et al*., 2007; Levin and Cotton, 2008). 2D simulations by Lynn *et al*. (2007) on mixed-phase clouds suggested that there is a decrease of orographic precipitation if the background aerosol conditions changed from maritime to continental. Niyogi *et al*. (2007) showed that aerosols influence the albedo impacting land surface processes. The land surface processes also play an important role in the monsoonal rainfall. An increase in aerosol number concentration is assumed to retard the cloud droplet coalescence and the riming process in mixed-phase orographic clouds and thereby decreasing orographic precipitation (Muhlbauer and Lohmann, 2009). Recently Singla *et al*. (2017) made a CCN closure study at MBL. They studied the bulk composition of aerosols and suggested that (a) size and chemical composition play an important role in particle activation, (b) even a small fraction of inorganics is sufficient for activating the aerosol particle and converting it into CCN and (c) replacing the contribution of organics with water-soluble Oxygenated Organic Aerosol give better results in CCN closure study.

The WG mountain range is located along the western coast of peninsular India. It extends approximately from 12° N to 20° N and from 73° E to77° E. The present study region is a square of side 600 km with MBL (17.92° N, 73.66° E) at its centre. MBL is a place in the WG region with a maximum height of 1439 meters at its highest peak above mean sea level. It is a vast plateau measuring 150 km^2 (58 sq mi), bound by valleys. The mean topography of the region of study is shown in Fig. 1. In this work, data collected during the 2015 monsoon season,

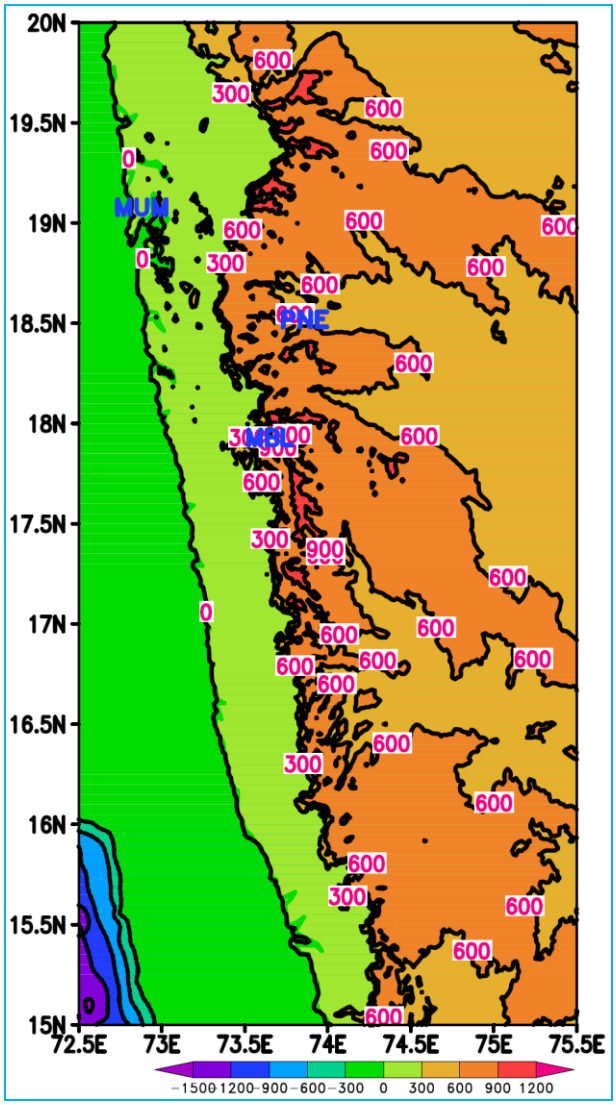

Fig. 1. Orography over and around the study location

i.e., June-September, 2015 (SWMS), was analyzed to study (*i*) the fluctuations in the daily rainfall, (*ii*) to understand the contribution of orographic and convective rainfall deduced from respective models over MBL, (*iii*) to study the influence of aerosol and the contribution of large scale synoptic systems on the variability of station's rainfall.

The characteristics of the rainfall over Mahabaleshwar [MBL, the high altitude station in the Western Ghat (WG) region] have been discussed in this study. Although MBL being on the windward side of WGs of the Indian sub-continent, receives its rainfall mainly due to orography, an attempt has been made here to find out the contribution of convection (if any) also in the total rainfall over the study station. The estimated rainfall produced by orographic and convective models has been compared with the observed rainfall over the study location. Over MBL, it is seen that high and low rainfall episodes are frequently observed during monsoon season. The study of these episodes during monsoon 2015 considering the influence of synoptic-scale systems has also been discussed.

The paper is structured as follows : Section 2 describes the data used in the present study. Section 3 discusses the synoptic conditions prevailing over the study area during the study period. In section 4, the methodology for estimating convective and orographic rainfall using models developed by De and Dutta (2005) and Dutta (2007) respectively have been discussed in brief. Finally, we end with a discussion of our results in section 5 and the concluding remarks are given in section 6.

2. Data

The ERA-Interim data set is produced by European Centre for Medium-Range Weather Forecasts (ECMWF) and the daily reanalysis data have been retrieved using the link http://data-portal.ecmwf.int/data/d/ interim_full_daily / levtype=pl., (Dee *et al*. 2011). The data contained parameters, *viz*., geopotential height, *u* and *v* component of wind, relative humidity, temperature, dew point temperature at 1000, 925, 850,700, 600, 500, 400, 300, 250, 200, 150 100 hPa levels at 0000/1200 UTC with the resolution of 0.125° × 0.125° latitude/longitude grid. This data is used for estimating orographic rainfall using a 3-D dynamical model. The orographic model needs the vertical profile of undisturbed mean flow, which is constructed using data on the windward side at the far upstream location of the orographic barrier (in the present study, it falls over the Arabian sea) and the radiosonde data is not available there. Therefore, the dynamic model of orographic rainfall has been initialized using the ECMWF reanalysis data like wind, temperature and humidity on the windward side at the orographic barrier's far upstream location (100 km away from the MBL). This data is generated from surface to upper atmosphere by averaging over one point (100 km away in the west, from the station under study). The estimated rainfall intensity (RFI) has been compared with the daily observed rainfall data of MBL.

In situ radiosonde data over the study location, MBL is taken from the High Altitude Cloud Physics Laboratory (HACPL, IITM). This radiosonde data and ECMWF reanalysis data are used for estimating convective rainfall. Daily rainfall data for June-September 2015 of MBL

TABLE 1

Daily rainfall data for June-September 2015 of MBL (17.58° N, 73.43° E) from Indian Daily Weather Report (IDWR), IMD.

Dates	June 2015	July 2015	August 2015	September 2015
01	0	23.1	58	23.4
02	0	3.2	15.4	5.9
03	0	0	14.8	0.8
04	0	0	26	0
05	19.2	0.2	74.5	0
06	1.5	0	90.4	0
07	0	9.8	38.8	0
08	3	10.4	11.6	0
09	9.7	18.8	33	0.4
10	0.2	24.8	27.3	76.5
11	1.9	14.3	12.6	20.6
12	26.6	7.1	15.2	0.3
13	7.8	6.1	14.6	2.8
14	14.9	6.1	30.2	2.4
15	25.1	2.1	41.6	11.3
16	18.7	12.6	21.4	61.2
17	25.2	51.8	16.1	62.8
18	21	30.2	6.9	13.4
19	55.6	39.9	0	35.4
20	65.2	85.4	0	1.5
21	184	44.6	1.6	21
22	365.8	148	34.6	16.2
23	184	97.1	45.3	2.4
24	270.4	65.4	56.2	0
25	83.7	94.9	36.8	0
26	24.6	25.1	53.2	0
27	19	15	6.6	0
28	1.6	34.8	34.7	0
29	0.4	29.6	0	0
30	11.4	95.6	22.6	0
31	-	74.8	20.6	0

(17.58° N, 73.43° E) shown in Table 1 is collected from Indian Daily Weather Report (IDWR), IMD. Daily average Outgoing Longwave Radiations (OLR) data based on Mahakur *et al*. (2013) over the Indian region (40.0° S-40.0° N, 25.0° E-125.0° E) in regular latitude-longitude grid of resolution 0.25° × 0.25° degrees is also used (http://www.tropmet.res.in/~mahakur/ Public_Data/ index. php?dir=K1OLR%2FDlyAvg%2F). The aerosol size distribution and total concentration were measured with a Wide Range Aerosol Spectrometer (WRAS, GRIMM; EDM 665). WRAS is a combination of Aerosol particle sizer (APS) and Scanning Mobility Particle Sizer (SMPS) and it provides aerosol number concentration from 5.14 nm to 32 µm size. A CCN counter (CCN-100, DMT Inc.) was used to measure Cloud Condensation Nuclei (CCN) concentration at different supersaturations (0.1%, 0.3%, 0.5%, 0.7%, 0.9%). 5 day back trajectory data was generated using the Hysplit model (Draxler and Rolph, 2003) to ascertain airmass origin. The specific humidity at different pressure levels was obtained from ERA-interim (ECMWF).

3. Chief synoptic features during 2015

During the Monsoon season (2015), 11 LPS (low pressure and stronger systems) were formed. Out of these, 8 further intensified as Depression, deep depression, cyclonic storms against a normal of 4-6 Depressions during the season. Two of which intensified into cyclonic storm ‘Ashobaa’ (7-12 June) & ‘Kemon’ (26 July-2 August) over the Arabian Sea and Bay of Bengal respectively and three as Deep Depressions with 2 over land (27-30 July and 16-19 September) and one over Arabian Sea (22-24 June). The 3 Depressions of which 2 formed as land Depression over Jharkhand and neighborhood (10-12 July) and over East Madhya Pradesh and adjoining Chhattisgarh (4 August). The remaining formed over the Bay of Bengal (20-21 June). Out of 3 low-pressure areas, one intensified as a well-marked low-pressure area.

During the season, the two deep depressions occurred between 22-24 June (Arabian Sea) and 27-30 July (over Land), but both were short-lived and occurred over the northwestern part of India. These deep depressions remained active over the western and the north-western part of the country only. These depressions mostly gave localized heavy rainfall and failed to produce widespread rainfall over the country's core monsoon zone. So it is evident that monsoon 2015 mainly produced weather systems of a shorter time scale.

Despite all these synoptic systems, all India SWMS 2015 was deficient and was a year of mega El-Nino lead to less rainfall. The high and low rainfall epochs were observed during the season over MBL depicting the intra-seasonal variations. The study of two representative spells

(one high and one low rainfall) have been discussed here in detail.

3.1. *Case I : Synoptic condition during high rainfall spell (19-25 June, 2015)*

During this period, the rainfall over the station varied between 56 to 366 mm/day. As per, IDWR 2015, Monsoon Trough (MT) was either active at its normal position or was south of its normal position. The offshore trough was present from the South Gujarat coast to north Kerala coast throughout the study period. From 17th June onwards, Low (L) was present over the Bay of Bengal (BOB) region, which became Well Marked Low (WML) on the 19th and concentrated into Depression (D) on the 20th over the Northwest and adjoining west-central BOB. It weakened into WML on 22nd. At the same time, on 21st June, L was formed over the Northeast Arabian Sea (AS) off the Gujarat coast, which concentrated into D and Deep Depression (DD) on 22nd and 23rd June. On 25th, it weakened into D, then WML and L on the same day. All the conditions were conducive to the intense rainfall activity over the station.

3.2. *Case II : Low rainfall spell (1-7 July, 2015) Synoptic condition*

This period recorded the rainfall from trace (0) to 24 mm/day over the study location. During this period, monsoon trough was oscillating between the foothills of Himalaya and its normal position, but most of the time it was at the foothills of Himalaya. Although on 30th June there was L present over east UP and adjoining north MP, it became less marked on 1st July. The feeble offshore trough was present from 30th June to 3rd July but was absent from 4th July onwards for the remaining period, *i.e.*, up to 7th July. Weak Cyclonic circulations were present over the BOB region and the southwest monsoon was subdued over Konkan & Goa, Madhya Maharashtra region during this period (IDWR, 2015). All these synoptic conditions were responsible for the low rainfall activity over the station.

4. Methodology

In this section, orographic and convective precipitation have been estimated using Dynamical models for orographic precipitation (Dutta, 2007) and Convective precipitation model (De & Dutta, 2005). In both the models, there are two parts, *viz.*, updraft estimation (orographic or convective) and rainfall intensity (RFI) estimation. In the following subsections, orographic and convective updrafts estimation, followed by RFI estimation, have been discussed.

4.1. *Estimation of orographic updraft*

Sarker *et al*. (1966, 1967) proposed a 2-D dynamical model for diagnosing orographic rainfall due to the flow of moist air across the Mumbai-Pune section of the Western Ghats. Dutta (2007) developed a 3-D mesoscale dynamical model for diagnosing orographic rainfall due to a basic flow of moist air across the orographic barrier and it was applied to the Western Ghats. To run both the above models, vertical profiles of horizontal wind, temperature, pressure and humidity are required and they were constructed using observed RS data of Santacruz, Mumbai. Orographic updraft in the present study has been computed following the dynamical model Dutta (2007). However, in the present study,vertical profiles of horizontal wind, temperature, pressure and humidityat far upstream location have been constructed using ECMWF high (0.125° × 0.125°) resolution reanalysis data. The model considers an adiabatic, inviscid, non-rotating and Boussinesq flow under steady-state condition across a mesoscale 3-D orographic barrier. Realistic vertical variation of prevailing wind speed and stability is allowed. The basic flow is also assumed to have both components, *viz*., normal and parallel to the major ridge of the barrier. For simplicity, the 3-D orographic barrier is assumed to have an elliptical contour, with major ridge being normal to the basic flow. Here, the *x*-axis is taken along the basic flow, the *y*-axis in the cross-flow direction and the *z*-axis vertically upward. The 3-D elliptical barrier is analytically expressed as :

$$h(x,y)=\frac{H}{1+\left(\frac{x}{a}\right)^2+\left(\frac{y}{b}\right)^2} \tag{1}$$

where, H is the maximum height of the elliptical barrier and a and b are the half widths of the elliptical barrier along the minor and major ridge axes, respectively. In the present study, following Dutta (2007) we have taken a = 18 km, b = 2.5a = 45 km and H = 0.77 km. Under the above assumptions, the Governing equations have been simplified and the simplified governing equations are linearized using perturbation techniques. As the height of the barrier in this study is approximately 1 km and the basic flow is saturated with a moist-adiabatic lapse rate, hence the linear study is justified (Rotunno and Ferretti, 2001). Linearized equations have been subjected to double Fourier transformation according to the formula:

$$\hat{f}(k,l,z)=\frac{1}{4\pi^2}\int_{-\infty}^{\infty}\int_{-\infty}^{\infty} f(x,y,z)\,e^{-i(kx+ly)}\,dx\,dy \tag{2}$$

where, $\hat{f}(k,l,z)$ is the double Fourier transform of *f*(*x*, *y*, *z*). The Fourier transformed equations, after some algebraic simplification, are reduced to the following vertical structure equation:

$$\frac{\partial^2 \hat{w}_1}{\partial z^2} + \left[\frac{N_m^2\left(k^2+l^2\right)}{\left(Uk+Vl\right)^2} - \left(\frac{k\frac{d^2U}{dz^2} + l\frac{d^2V}{dz^2}}{kU+lV} \right) - \frac{1}{\rho_0}\frac{d\rho_0}{dz}\left(\frac{k\frac{dU}{dz} + l\frac{dV}{dz}}{kU+lV} \right) - \left(k^2+l^2\right) + \frac{1}{4\rho_0^2}\left(\frac{d\rho_0}{dz}\right)^2 - \frac{1}{2\rho_0}\frac{d^2\rho_0}{dz^2} \right] \hat{w}_1 = 0 \quad (3)$$

where, $\rho_0(z)$ is basic state density, $\tilde{w} = (k,l,z)$ is the 2-D Fourier transformation of perturbation vertical velocity $w' = (x,y,z)$ and $\tilde{w}_1 = (k,l,z) = \sqrt{\frac{\rho_0(z)}{\rho_0(0)}}\,\tilde{w}(k,l,z)$.

Considering the second order of smallness of the last two terms within parenthesis, the equation (3) further simplified to

$$\frac{\partial^2 \tilde{w}_1}{\partial z^2} + \left[f(k,l,z) - \left(k^2+l^2\right) \right] \tilde{w}_1 = 0 \quad (4)$$

where,

$$f(k,l,z) = \left[\frac{N_m^2\left(k^2+l^2\right)}{\left(Uk+Vl\right)^2} - \left(\frac{k\frac{d^2U}{dz^2} + l\frac{d^2V}{dz^2}}{kU+lV} \right) - \frac{1}{\rho_0}\frac{d\rho_0}{dz}\left(\frac{k\frac{dU}{dz} + l\frac{dV}{dz}}{kU+lV} \right) \right] \quad (5)$$

$$\text{where, } N_m^2 = \frac{g}{\beta\overline{\theta_e}\left(1+q_s\right)}\frac{d\overline{\theta_e}}{dz} \ldots. \quad (6)$$

$$\text{and } \beta = 1 - \frac{Lq_s}{C_p\overline{T}}\left(\frac{\varepsilon+\gamma q_s}{\varepsilon+q_s}\right) \ldots. \quad (7)$$

where, γ is the ratio between two specific heats of gas, ε is the ratio between dry and moist gas constants and q_s is the basic state saturated mixing ratio of water vapour.

Following Dutta (2007), equation (4) is solved quasi-numerically for $\tilde{w} = (k,l,z)$ using following boundary conditions:

(*i*) Lateral boundary condition is periodic

(*ii*) At the lower boundary, *i.e*., at the surface (*z* = 0) airflow is tangential to the ground surface.

(*ii*) Above the upper boundary basic flow was assumed to be neutrally stratified with a constant velocity. Thus, in the above model it was assumed that above the upper boundary, $f(k,l,z) \approx 0$, which implies that at and above the upper boundary, $\tilde{w}_1 = (k,l,z) \propto e^{-KZ}$. Since the pressure, vertical velocity are continuous functions of *z*, therefore, $\tilde{w}_1, \frac{\partial \tilde{w}_1}{\partial z}$ are also continuous functions of *z*. Hence, above the upper boundary, $\frac{\partial \tilde{w}_1}{\partial z} = -K\tilde{W}_1$. These two equations provided upper boundary conditions in the above model.

After computing $\tilde{w} = (k,l,z)$ for all permissible wave number vectors (k,l) at each model vertical levels (two successive levels separated by 0.25 km), perturbation vertical velocity $w' = (x,y,z)$ is computed by performing inverse 2-D Fourier transform, following Dutta (2007). For more details, Dutta (2007) may be referred.

4.2. *Estimation of Convective updraft*

Convective updraft at each level has been estimated following De & Dutta (2005). The same technique was used by Dutta *et al*. (2015), while studying the role of convective instability on heavy rainfall over Sylhet, Bangladesh, on an isolated day.

For the computation of convective rainfall intensity, a vertical profile of temperature, humidity and pressure data are required. These may be obtained from station RS data, or it can be constructed using reanalysis (*e.g*., ECMWF, NCEP/NCAR, etc.) data at different levels. As the study of De and Dutta (2005) addressed convective precipitation over Santacruz (SCZ) and it is a RS station, RS data of SCZ were used. However, in the study of Dutta *et al*. (2015), the vertical profile of

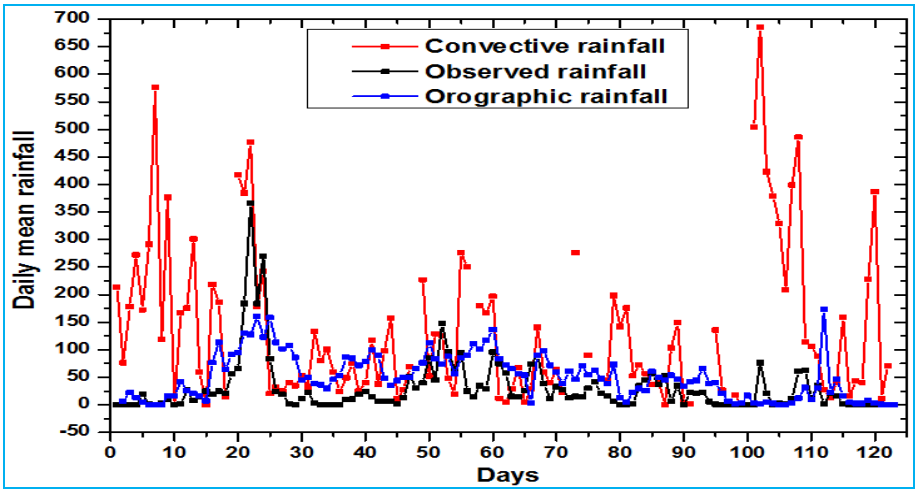

Fig. 2. The daily variation of the observed and the estimated rainfall usingconvective and orographic models over the study location for the year south west monsoon 2015

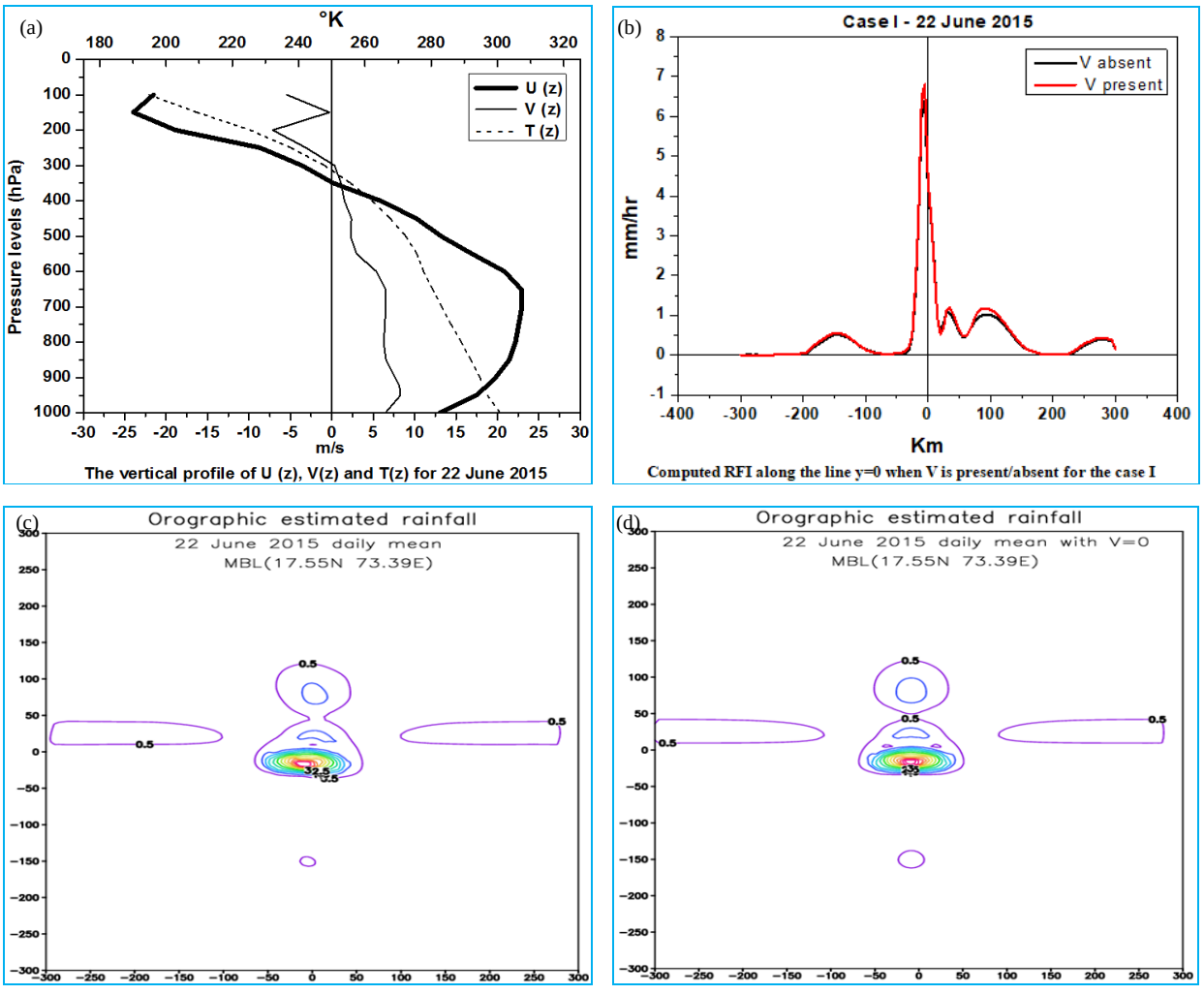

Figs. 3(a-d). (a) Vertical profile for U, V and T for 22 June, 2015, (b) The Rainfall Intensity, RFI (mm hr^{-1}) map for 22 June, 2015, (c) Estimated orographic rainfall using model for 22 June, 2015 and (d) Estimated orographic rainfall using model when V = 0 for 22 June, 2015

pressure, temperature and humidity for the station Sylhet was constructed using ERA 40 data, as RS data for Sylhet was not available. In this study, the vertical profile of these variables have been constructed using RS data of MBL(when it was available) as well as the same was constructed using ECMWF high (0.125° × 0.125°) resolution reanalysis data. Using the vertical profile of the above-mentioned variables over MBL and the algorithm developed by Krishnamurti (1986), the virtual temperature of the environment and that of air parcel have been obtained and then at each discrete pressure level '*i*', the value of buoyancy force B_i is computed. Using these values of B_i, convective updraft at each level is computed (may be referred to De and Dutta 2005 for further details). Rainfall Intensity (RFI) is computed using both data sets. But due to the lack of continuous radiosonde data, the estimated rainfall using ECMWF data only is presented here and compared with observed rainfall.

4.3. *Estimation of orographic precipitation and convective precipitation rates*

Using the inputs, *viz*., vertical velocity (*w*), the density (*r*) and saturation-mixing ratio (*q*) following Sarker (1966, 1967), rainfall intensity due to the net convergence in the layer bounded by the i^{th} pressure level and $(i + 1)^{th}$ level is given by

$$R_i = \left[w_i\rho_i\left(q_i - q_m\right) + w_{i+1}\rho_{i+1}\left(q_m - q_{i+1}\right)\right] \times 0.036 \text{ mm/hr}.. \quad (8)$$

where, w_i, ρ_i, q_i are respectively the vertical velocity (due to orographic updraft or convective updraft), saturation mixing ratio and density at i^{th} pressure level and $w_{i+1}, \rho_{i+1}, q_{i+1}$ are those at $(i + 1)^{th}$ level, $q_m = \frac{q_i + q_{i+1}}{2}$ and R_i is the rainfall intensity due to the net convergence in the layer bounded by the i^{th} pressure level and $(i + 1)^{th}$ level. Hence the convective rainfall intensity obtained from the column up to level of neutral buoyancy is $\sum_1^{N-1} R_i$ mm/hr. In the above summation, we have taken $R_i = 0$ if $R_i \le 0$. While computing orographic rainfall rate at each point, perturbation vertical velocity, due to orographic updraft at each point has been considered and also the effect of wind drift has been incorporated, following Dutta (2007).

5. Results and discussion

It is well known that the region on the windward side of WG receives more frequent and heavy rainfall due to the orography. If orography is the only cause for this, then the region on the windward side of WG should get continuous and heavy rainfall, but it is seen that the rainfall over MBL has noticeable variability. The possible causes for this variability have also been tried to address in this study.

In this section, rainfall characteristics over the station MBL for the entire season have been discussed along with the probable factors responsible for its intra-seasonal variations during June-September 2015. The two rainfall spells, *viz*., from 19 to 25 June. (High rainfall spell, Case I) and 1 to 7 July. (low rainfall spell, Case II) 2015, have been studied and discussed in detail. Fig. 2 shows the daily variation of the observed, the rainfall estimated from the convective and orographic model over the study location for the period June-September 2015.

5.1. *Computation of orographic rainfall intensity in different cases*

The orographic RFI (in mm hr^{-1}) has been computed in the study (WG) region using the above 3-D model. After computing RFI, map of RFI and RFI distribution in the central plane along $y = 0$ have been prepared for all cases. In these maps, contours of RFI are separated by an interval of 0.4 mm hr^{-1}. The 3-D profile of the WG is expressed by Eqn. (1), with a = 18 km, $b = 2.5a$ = 45 km and H = 0.77 km. In the present study, the MBL section of the WG is taken as the central plane ($y = 0$).

As a representative case, two rainfall epochs (high and low) have been studied in detail and out of that two representative days are selected and discussed here in detail.

Case I : *22 June, 2015 : High rainfall day*

High-resolution ECMWF reanalysis data near MBL (100 km away on the western side) for the JJAS period has been used in this case. The vertical profiles of $U(z)$, $V(z)$ and $T(z)$ for 22 June are shown in Fig. 3(a). 22 June was the day when the observed rainfall over the site was 365.8 mm. Vertically averaged value of U is 8.58 ms^{-1} whereas that of V is 3.14 ms^{-1}. The averaged values suggest the strong south-westerly flow on 22 June. Computed RFI along the line $y = 0$ when "*V*" is present as well as when "*V*" is absent for the case I (22 June, 2015) have been shown in Fig. 3(b). The figure depicts that the maximum RFI in the central plane occurs not on the peak of the barrier but slightly to the windward side of the peak and is in agreement with radar observations of rainfall over this region, Utsav *et al*. (2017). It can also be seen that when "*V*" is absent, the computed RFI maxima in the central plane occurs at about 5 km upstream of the peak of

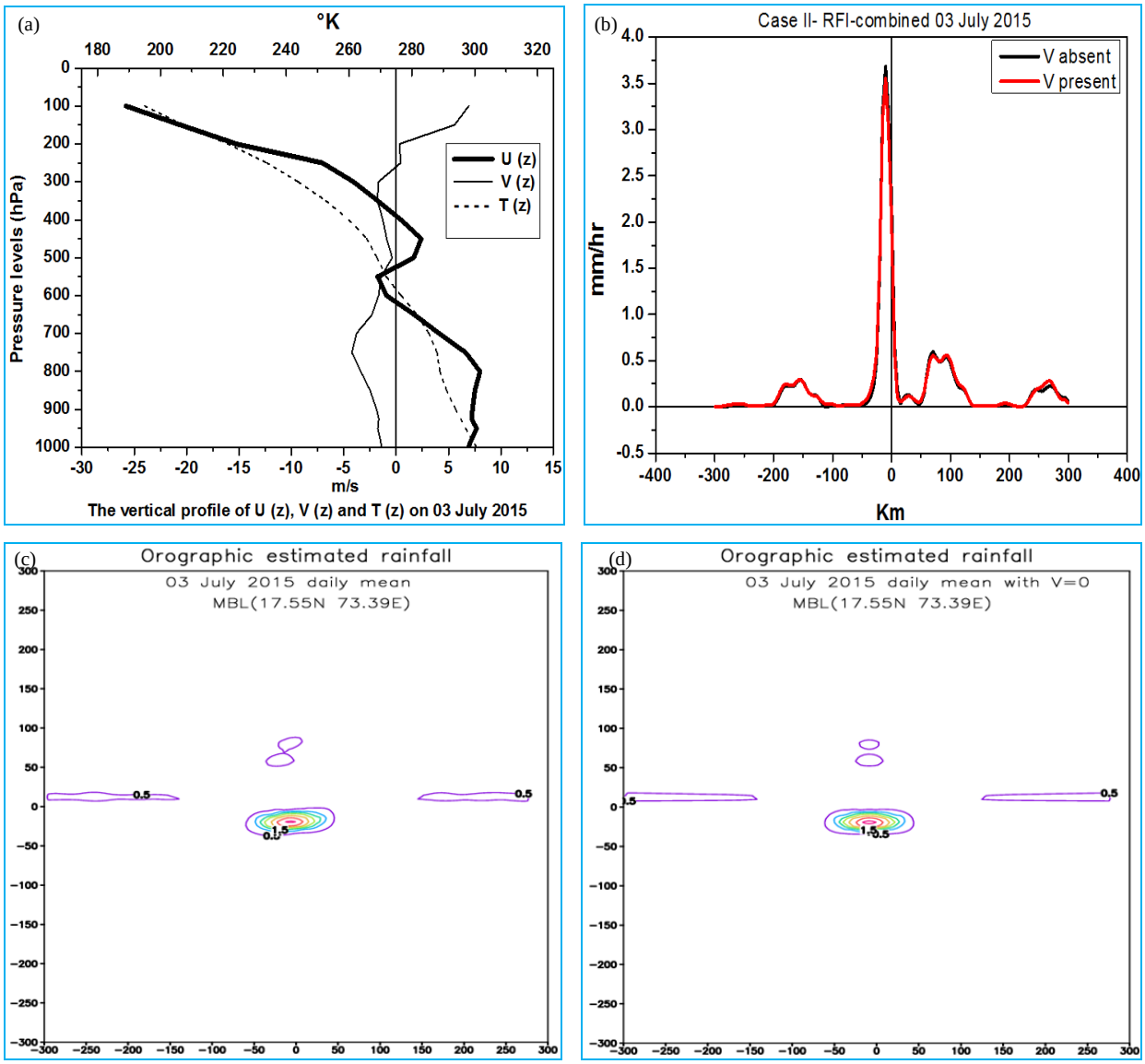

Figs. 4(a-d). Same as Figs. 3(a-d) but for 3 July, 2015

the barrier and the value of the maxima is 6.38 mm hr^{-1}. Whereas, in the presence of "*V*" the computed RFI maxima also occurs at 5 km upstream of the barrier with an enhanced magnitude of 6.8 mm hr^{-1}. The observed RFI was estimated to be 13.2 mm hr^{-1} at MBL. The maps of computed RFI on the horizontal plane are shown in Figs. 3(c&d) for the situations when "*V*" is present or absent respectively. In Fig. 3(d), there are five regions of RFI maxima, the primary one being located to the windward side in the central plane. Two secondary maximas were present with less intensity, in the central plane located from 85 to 285 km (elongated) away from the peak on the leeward and windward side. The other two secondary maximas are located, one near the flank of the barrier on the windward side at y = 100 km with maximum intensity and another with less intensity at y = –150 km. In Fig. 3(c), also there is one primary maxima and four secondary maximas in the RFI, but the symmetry in the locations of secondary maxima about the central plane (y = 0 km) is no longer present in the presence of "*V*" component.

Case II : *3 July, 2015 : Low rainfall day*

The vertical profiles of $U(z)$, $V(z)$ and $T(z)$ for the case II, *i.e.*, 3 July, 2015 are shown in Fig. 4(a). The observed rainfall over the site was 00.00 mm on this day. Vertically averaged value of U is -0.78 ms^{-1} whereas that

of *V* is -0.93 ms^{-1} depicting the dominance of easterly and northerly components of wind. This further suggests that the south-westerly monsoon flow was very weak on this day. Computed RFI along the line y = 0 when "*V*" is present as well as when "*V*" is absent for the case I (3 July, 2015) have been shown in Fig. 4(b). The figure depicts that the maximum RFI in the central plane occurs not on the peak of the barrier but slightly to the peak's windward side. It can also be seen that when "*V*" is absent, the computed RFI maxima in the central plane occurs at about 10 km upstream of the peak of the barrier and the value of the maxima is 3.69 mm hr^{-1}. Whereas, in the presence of "*V*" the computed RFI maxima occurred at 10 km upstream of the barrier with the value almost the same as 3.56 mm hr^{-1}. The observed RFI was almost 0 mm hr^{-1} at MBL. The computed RFI maps on the horizontal plane are shown in Figs. 4(c&d) for the situations when "*V*" is present or absent respectively. In Fig. 4(d), there are four regions of RFI maxima, the primary one being located to the windward side in the central plane, two secondary maximas with less intensity, in the central plane located from 125 to 300 km (elongated) away from the peak on the leeward and windward side and other secondary maxima is located near the flank of the barrier on the windward side at y = 75 km. In Fig. 4(c), also there is one primary maxima and three secondary maximas in the RFI, but the symmetry in the locations of secondary maxima about the central plane (y = 0 km) is no longer present in the presence of "*V*" component. The above description of high and low rainfall days suggests that the orographic model produced the rainfall intensity comparable to the observed rainfall. From the above cases (I and II), it can be seen that the estimated rainfall (6.38 & 6.8 mm hr^{-1}) is underestimating when there is more rainfall (13.2 mm hr^{-1}) but it is seen to be overestimating (3.69 & 3.56 mm hr^{-1}) when there is less rainfall spell (0.0 mm hr^{-1}) over the study location.

5.2. *Contribution of convective instability in the rainfall intensity*

Initially, the comparison is made between the observed rainfall and the rainfall estimated from the convective model and the comparison of orographic rainfall is done in the subsequent section. From Fig. 2, it can be seen that the daily observed and the estimated rainfall using the convective model are not matching with each other proving the inefficiency of the model over the orographic station. It is also seen that the estimated rainfall is overestimating the observed rainfall. This may be attributed to advection, in-situ change in vertical velocity (w), the entrainment effect, the effect of compensating downward motion and the effect of friction that have not been incorporated in the computing model the convective rainfall intensities. It can be concluded that the present convective rainfall model was not able to depict the observed rainfall but was able to capture the fluctuations in the observed daily rainfall. While studying the various epochs of rainfall events, it is noticed that the rainfall over MBL has also been affected by some other factors like large scale synoptic systems present over BOB, presence and position of monsoon trough and the presence of offshore trough. But it is also seen that sometimes there are events of good rainfall over the location in the absence of any marked synoptic systems, which may be due to the station's orography.

It can be seen from Fig. 2 that the estimated values of rainfall from the convective model are overestimating the rainfall in magnitude, but in the general model was able to capture the variations in the daily observed rainfall intensities. It can be inferred that even in the WG region, there are sudden variations of rainfall and that may be due to the interaction between orographic forcing and convective instability.

5.3. *Experiment using vertical velocity* (w) *from orographic rainfall model*

In the convective model, the value of w is taken as zero at Level of Free Convection (LFC). Initially applying the same, *i.e.*, w = 0 at LFC, the values of RFI were computed and the same is presented in Fig. 2. These values of RFI are seen to be overestimated when compared with observed rainfall. For releasing convective instability a certain lifting of air parcel up to the LFC is required, which may be triggerred by orographic lifting (De and Dutta, 2005). Therefore, to study the role of an orographic accent to trigger convection and improve the computed convective precipitation estimation, an experiment was carried out. Initially, from the orographic model, the value of w at LFC was extracted. These values of w at LFC were put in the convective model instead of putting its valuezero at LFC. The experiment was carried out for the two rainfall episodes. Although it is seen that there is no marked difference in the values of RFI during these periods, but the results seem to be encouraging and it is felt that this exercise should be carried out for more number of cases for more robust results.

After assessing the performance of the two models, rainfall variability over the station (which is studied and discussed here) with respect to various parameters are discussed below.

5.4. *Rainfall and OLR*

It is well known that Outgoing Longwave Radiation (OLR) is used as a measure of convection over the region,

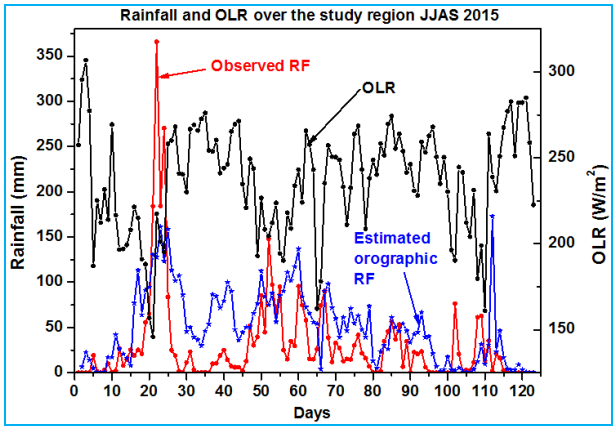

Fig. 5. The daily variation of observed, estimated orographic rainfall and OLRfor SWMS 2015

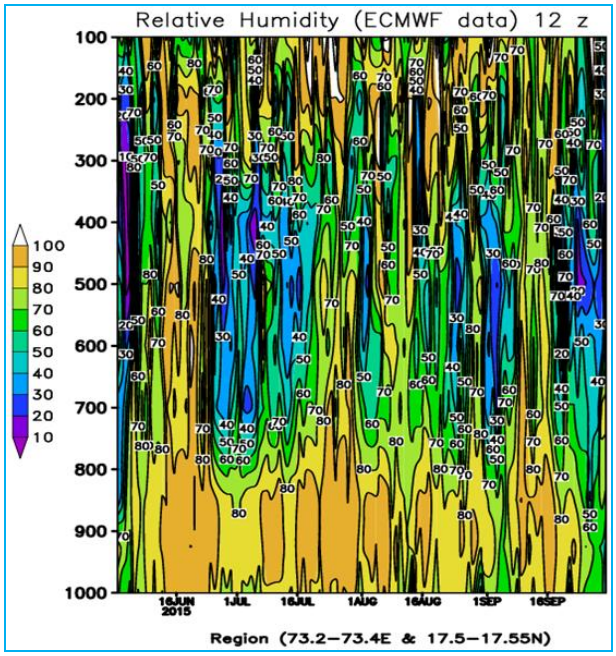

Fig. 6. Time series of RH (%), vertically integrated in the atmosphere (1000-100 hPa) for JJAS 2015 season at 1200 UTC

which ultimately can suggest the probability of occurrence of rainfall. The observed rainfall, estimated orographic rainfall and OLR for SWMS 2015 are plotted in Fig. 5. The observed rainfall shows a skewed distribution indicating the dominance of rainfall lesser than 100 mm day^{-1} category. When compared with the observed rainfall series, it is seen that even deeper clouds with OLR less than 180 Wm^{-2} did not produce many heavy rainfall events and *vice versa*. These observations warrents the need for further analysis of why the deeper convection did not produce heavy rainfall events over the station. Have aerosols played their role? An attempt has been made here to address this issue in the next section. From Fig. 5, the intraseasonal variation of rainfall and OLR in the SWMS of 2015 can be seen. As expected, they are in opposite phase with each other in most of the cases. In few occasions, despite the occurrence of rainfall, it is seen that there is not much decrease in the amount of OLR. The mismatch between rainfall and OLR might be because of their computational method, as the observed rainfall is a single point observation. Whereas OLR is the averaged estimation over the region near a location. Although OLR data is over high resolution (0.25 × 0.25 Lat. / Long. grid), the clouds that have produced rainfall might have a short life span and a smaller dimension in such cases. This observation is in line with the earlier studies by Konwar *et al*., 2014; Kumar *et al*., 2014. They have concluded that due to the forced condensation because of orography, shallow clouds precipitate heavily in WGs, much decrease in the values of OLR is not seen.

5.5. *Humidity and rainfall*

The surface level moisture is the key thermodynamic parameter. The time series of RH (%), vertically integrated with the atmosphere (1000-100 hPa) for the JJAS 2015 season at 1200 UTC, is shown in Fig. 6. The large fluctuations are seen on day to day time scales. In the analysis, it is seen that RH increases from about 60% in Jun to about 90% in Jul. and Aug. There are only 25% of the days when the RH is above 90%. These days are associated with LPS over the Bay of Bengal. Thus the surface conditions may be characterized as moist type similar to over the Arabian Sea as reported by Maheskumar *et al*. (2014). Throughout the season (JJAS, 2015), it is seen that there was sufficient moisture (> 90%) in the atmosphere up to 850 hPa, with one or two exceptions (start of the season, *i.e*., June and 1-9 September). There are some periods when RH values have increased (>90%) in the upper troposphere. It is found that this is because of the presence of synoptic systems (semi-permanent and transient), which had an influence on the moisture content over the study location and ultimately have increased the rainfall amount over MBL. The analysis is consistent with the observed rainfall (Fig. 2). During the high rainfall spell, the values of RH over the study region are seen to be increased (90%) and seen to be penetrating in the upper troposphere, whereas in the low rainfall spell percentage of more RH over the study region is seen to be confined up to lower troposphere.

The INSAT-3D satellite imageries for 22 June and 3 July are also produced in the Figs. 7 (a&b) represents the high and low rainfall spells during the study period.

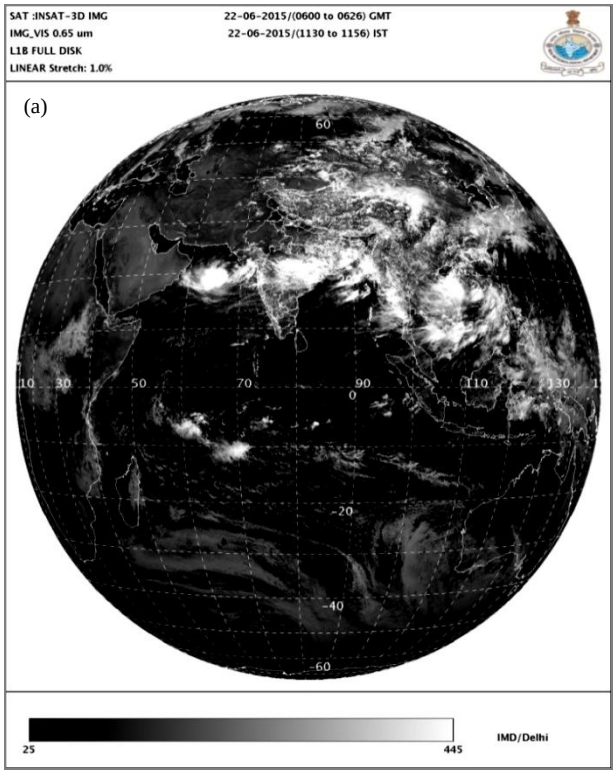

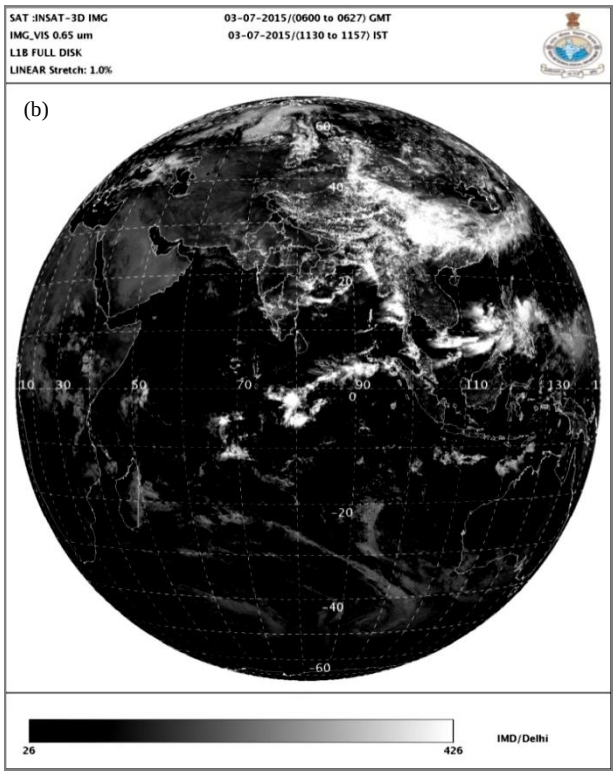

Figs. 7(a&b). (a) Satellite cloud picture for 22 June, 2015 (high rainfall day) and (b) Same as Fig. 8(a) but for 3 July, 2015 (Low rainfall day)

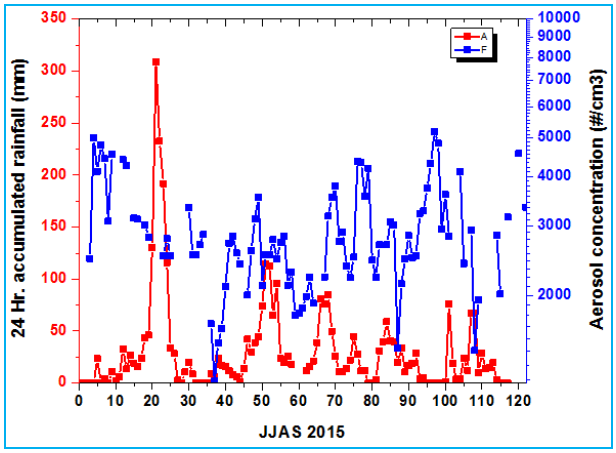

Fig. 8. Time series of the observed rainfall and the concentration of aerosols over the station

Fig. 7(a) shows the Indian region full of clouds depicting high rainfall spell, whereas Fig. 7(b) represents the low rainfall spell with clear sky condition.

5.6. *Possible influence of aerosols on the orographic rainfall*

In order to understand the possible effect of atmospheric aerosols on the orographic rainfall over this region, we utilized the collocated measurements of aerosol and CCN characteristics along with precipitation. Fig. 8 shows the time series of the observed rainfall and aerosols' concentration over the station (MBL). As already mentioned in the data section, the RF data is taken from the India Daily Weather Report, India Meteorological Department. The aerosol data is from a Wide Range Aerosol Spectrometer (Grimm). The cloud condensation nuclei (CCN) data was taken from the CCN counter (DMT) of the High-Altitude Cloud Physics Laboratory at the same location. All instruments are situated at the station. Previous studies from this site clearly indicated that despite the wet scavenging of aerosol due to rain spells during monsoon season, the aerosol concentration at the surface level shows high diurnal variability (Leena *et al*., 2016). There are local emissions, particularly in the monsoon season, contributing to the large diurnal variability in aerosol and CCN concentration. A recent study on the precipitation susceptibility over this site indicated that the moderate liquid water content clouds are highly susceptible to aerosols (Leena *et al*., 2018).

As the Western Ghat region is covered by dense forest, there could be a large contribution of secondary organic aerosols from the oxidation of volatile organic compounds (VOC), which could serve as a CCN which needs to be ascertained. It can be seen from Fig. 9(a) that there is a very minimal effect (uncorrelated) of rainfall on

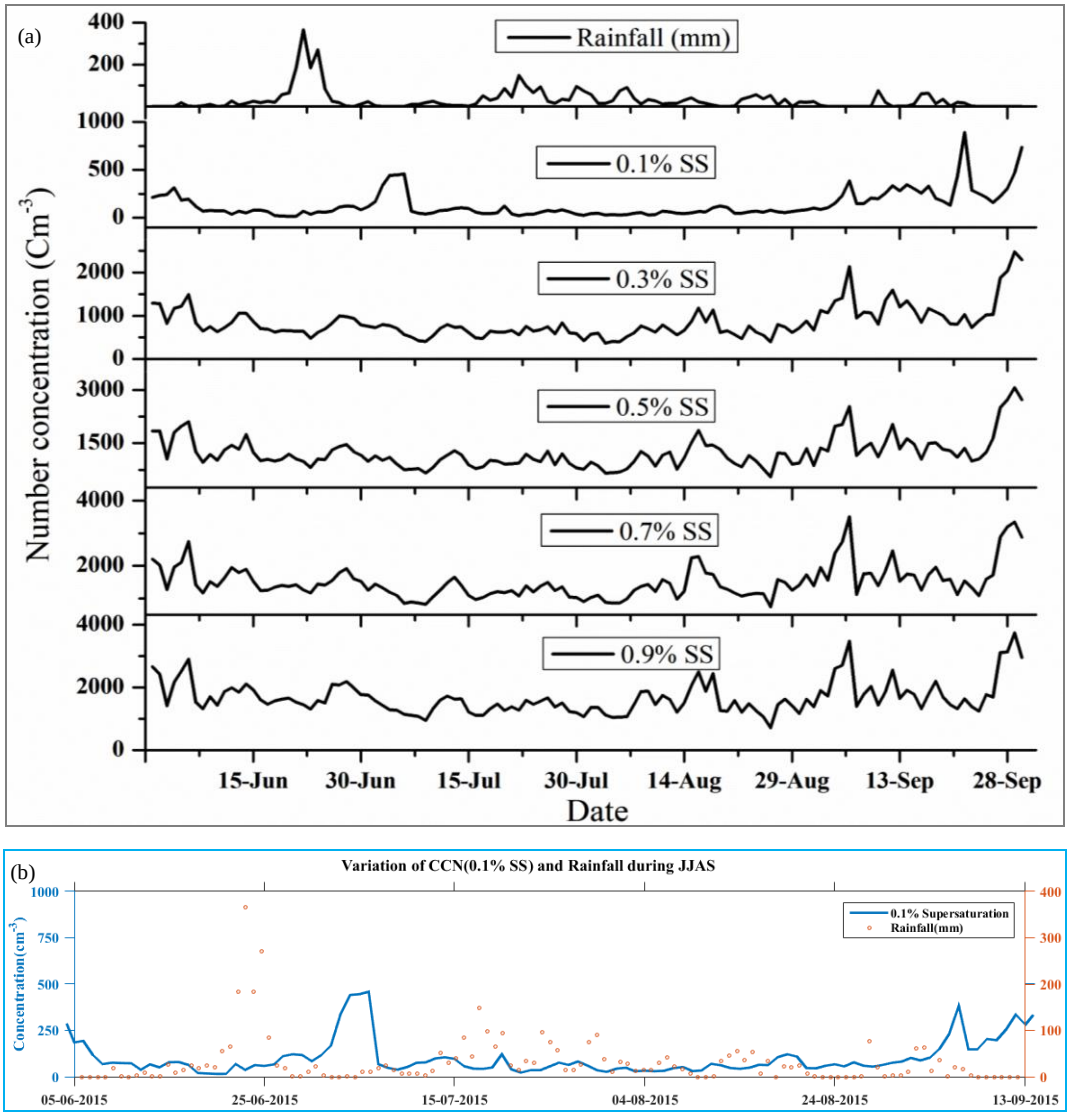

Figs. 9(a&b). (a) Daily variation of rainfall and number concentartion of CCN at various super saturation levels and (b) Same as Fig. 9(a) but only at 0.1% super saturation level

CCN concentration at supersaturation (SS) from 0.3% to 0.9% but there exists an inverse relationship between CCN at 0.1% SS and rainfall, Fig. 9(b). It is highly debatable that the enhancement of CCN at low SS (detectable particle size generally >250 nm at 0.1% SS; Singla *et al.*, 2017), during the break phase (1-7 July, 2015), is an artifact of less rain (low wet scavenging). Particles with this size range can act as very good cloud condensation nuclei (Activation efficiency is ~ 100%). These particles can modify the cloud size distribution spectrum, enhance the cloud reflectivity and negatively affect the rainfall process (Anil Kumar *et al.*, 2016). This phenomenon, in turn, may extend the break phase as to overcome this effect, more pool of moisture is needed (strong westerly). Air masses' back trajectories were analyzed using an HYSPLIT model for the active (high rainfall) and the break phase (low rainfall) periods at different height levels to ascertain aerosols' influence. The graph [Figs. 10(a&b)] shows a clear demarcation of air mass origin at 5000 m AGL (above ground level) for the active and break phase period. Air mass origin is mostly from the sea during the active phase and mostly from land during the break phase, although air mass is the sea at 1500 m AGL, Figs. 11(a&b). This observation depicts when the back trajectories are from the continent, there is a reduction in precipitation. Whereas the back trajectories from the ocean can bring hygroscopic giant CCN such as sea salt, which can enhance the collision-coalescence process and helps warm rain precipitation process, Maheskumar *et al.* (2014). An attempt is being made to

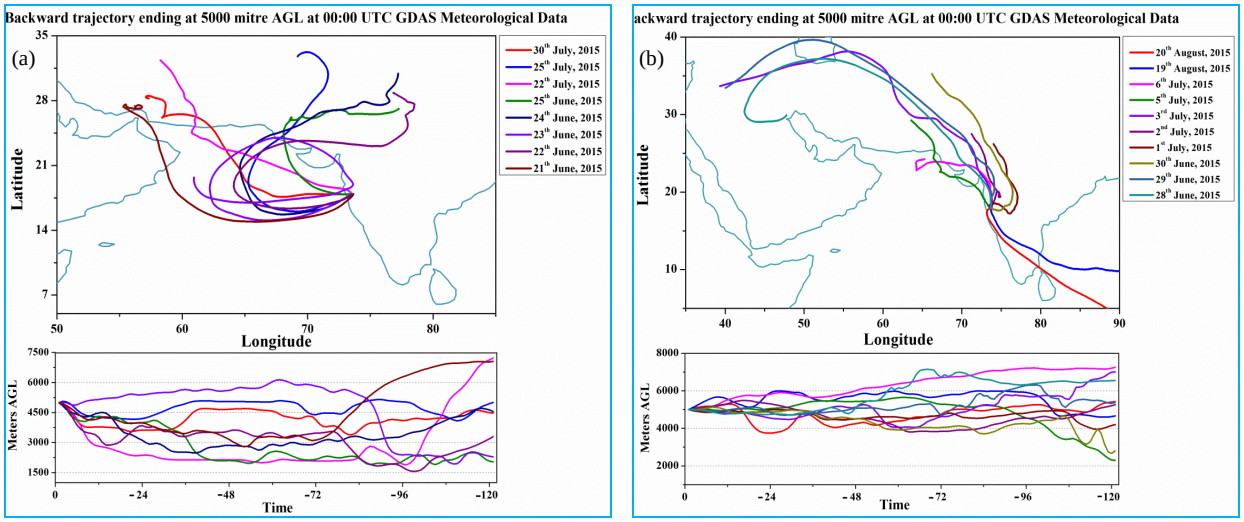

Figs. 10(a&b). (a) Backward trajectory ending at 5000 meter above ground level at 0000 UTC using GDS meteorological data during active phase period and (b) Same as Fig. 10(a) but during break phase period

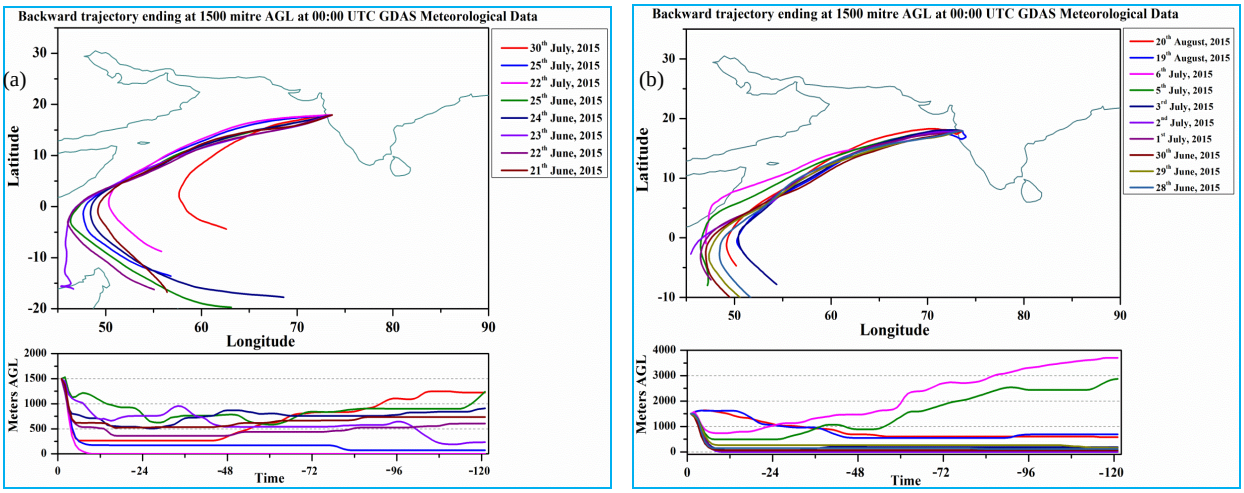

Figs. 11(a&b). (a) Same as Fig. 10(a) but for 1500 meter above ground level and (b) Same as Fig. 10(b) but for 1500 meter above ground level

study the type of aerosols, their origin, their size, etc. to confirm their positive/negative impact on the rainfall. This observation, in turn, also depicts the importance of depth of westerly core on precipitation.

This phenomenon, in turn, may extend the break phase as to overcome this effect, more pool of moisture is needed (strong westerly). Air masses' back trajectories were analyzed using an HYSPLIT model for the active (high rainfall) and the break phase (low rainfall) periods at different height levels to ascertain aerosols' influence. The graph [Figs. 10(a&b)] shows a clear demarcation of air mass origin at 5000 m AGL (above ground level) for the active and break phase period. Air mass origin is mostly from the sea during the active phase and mostly from land during the break phase, although air mass is the sea at 1500 m AGL, Figs. 11(a&b). This observation depicts when the back trajectories are from the continent, there is a reduction in precipitation. Whereas the back trajectories from the ocean can bring hygroscopic giant CCN such as sea salt, which can enhance the collision-coalescence process and helps warm rain precipitation process, Maheskumar *et al.* (2014). An attempt is being made to study the type of aerosols, their origin, their size, etc. to

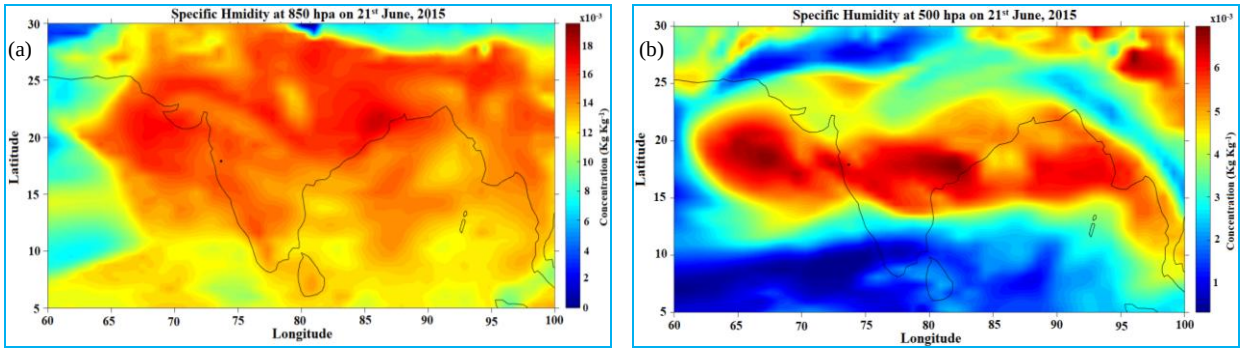

Figs. 12(a&b). (a) Specific humidity at 850 hPa for 21 June, 2015 and (b) Same as Fig. 12(a) but for 500 hPa

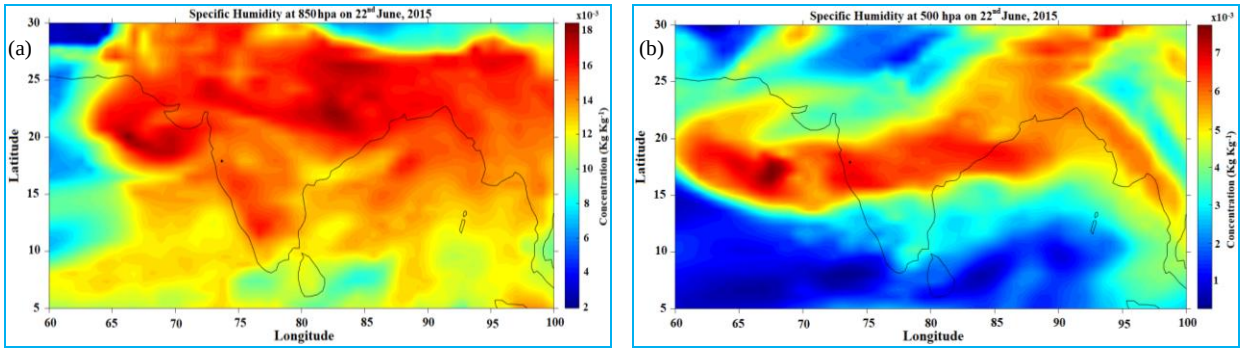

Figs. 13(a&b). (a) Same as Fig. 12(a) but for 22 June, 2015 and (b) Same as Fig. 12(b) but for 22 June, 2015

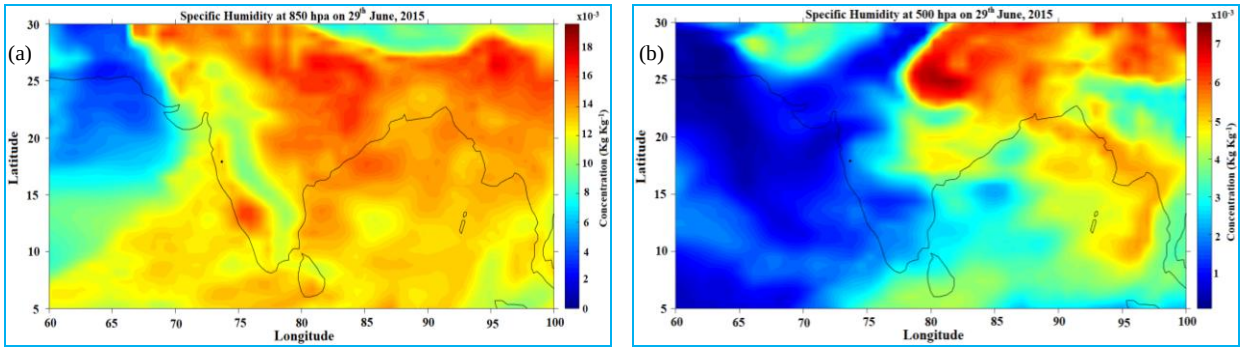

Figs. 14(a&b). (a) Same as Fig. 12(a) but for 29 June, 2015 and (b) Same as Fig. 12(b) but for 29 June, 2015

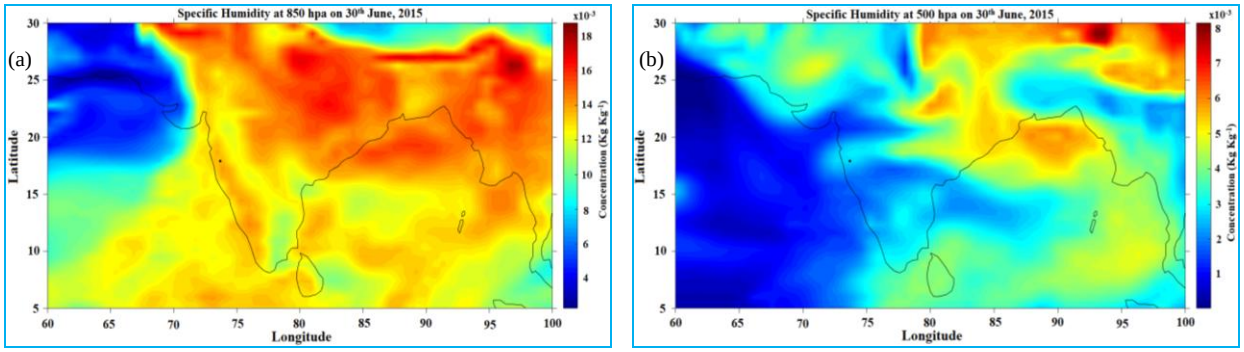

Figs. 15(a&b). (a) Same as Fig. 12(a) but for 30 June, 2015 and (b) Same as Fig. 12(b) but for 30 June, 2015

confirm their positive/negative impact on the rainfall. This observation, in turn, also depicts the importance of depth of westerly core on precipitation.

The spatial distribution of specific humidity at two representative levels, 850 and 500 hPa and for two days each for active and break phases over the study region are also presented. Figs. 12 (a&b) and Figs. 13(a&b) represents the active phase of rainfall over MBL observed on 21 and 22 June. Whereas Figs. 14 (a&b) and Figs. 15 (a&b) represents the break phase observed on 29 and 30 June, respectively. It is clearly visible that the depth of moisture extends up to 500 hPa during active phases, whereas the specific humidity is confined to lower-level during break phases.

6. Conclusions

An existing dynamical diagnostic model (Dutta, 2007) has been used to estimate the contribution of the orographic effect alone and an existing convective model (De and Dutta, 2005) has been used to estimate the contribution of convective instability alone to the observed rainfall over MBL region. In particular, the daily variation of the estimated orographic rainfall matches well with that of observed rainfall variability on a daily scale. From this study, it is seen that the performance of the convective model is not as good as that of the orographic model, which is obvious because the location under study is on the windward side of WG, but this convective model has proved its utility in earlier studies (De and Dutta, 2005) over other locations wherein orographic influence is less. The following conclusions can be drawn out from the study: The increase in the rainfall appears broadly due to the orographic, as the variation of estimated rainfall intensity computed using the dynamical model for orgraphic rainfall matches well with that of observed one. However, the estimated rainfall using orographic model is seen to be underestimated when there is heavy rainfall spell but it is overestimating when there is low rainfall spell over the study location.

(*i*) The increase in the rainfall appears broadly due to the orographic, as the variation of estimated rainfall intensity computed using the dynamical model for orographic rainfall matches well with that of the observed one. However, the estimated rainfall using the orographic model is seen to be underestimated when there is a heavy rainfall spell, but it is overestimating when there is a low rainfall spell over the study location.

(*ii*) The positive effect of the synoptic-scale systems on the rainfall over the station can be visualized by enhanced rainfall during the period. The rainfall in the absence of synoptic-scale systems is fetched due to the station's orographic location.

(*iii*) The rainfall contribution from the convective precipitation model into the total rainfall along with orographic rainfall at the station is noticed. Although it is difficult to quantify the same, it cannot be neglected.

(*iv*) Analyses of data for more years will be useful in quantifying the contribution from the convective and orographic rainfall at the station and surrounding region.

(*v*) There is an inverse relationship between CCN at 0.1% SS and rainfall. However, very minimal effect of rainfall on CCN concentration at supersaturation (SS) from 0.3% to 0.9% was observed.

(*vi*) The depth of moisture content has a positive impact on rainfall as it is observed to be low during the break phase (low rainfall) as compared to the active phase (high rainfall).

(*vii*) The high rainfall over the station is accompanied by the strong westerlies with depth up to 500 hPa level, whereas the low rainfall has westerlies confined up to 850 hPa.

(*viii*) Back trajectories depicted the presence of moisture-laden airmass consisting of giant CCN (sea-salt) when they are coming from the Arabian Sea and producing a good amount of rainfall. Whereas, when they are continental, they bring dry air from the desert area and limit the formation of rainfall.

(*ix*) Although the study is initially carried out using one-year data (2015), it is believed that it has brought out the location's rainfall characteristics so clearly that it can be considered as a representative over a longer time scale. Still, the findings from this study will be examined using data for more years.

Acknowledgments

The authors are grateful to the Director, IITM, Pune, India, for support and encouragement. IITM is fully funded by the Ministry of Earth Sciences, Govt of India. The authors also gratefully acknowledge the NOAA Air Resources Laboratory (ARL) to provide the HYSPLIT transport and dispersion model and READY website (https:// www.ready.noaa.gov) used in this publication. The authors gratefully acknowledge ECMWF for providing the ERA-Interim, Atmospheric model data. The authors also acknowledge NCEP/NCAR for the reanalysis data used in this publication. The authors are thankful to the anonymous reviewers for the very fruitful

comments/suggestions that were very useful to improve the paper's quality.

Disclaimer : The contents and views expressed in this research paper/article are the views of the authors and do not necessarily reflect the views of the organizations they belong to.

References

Anil Kumar, V., Pandithurai, G., Leena, P. P., Dani, K. K., Murugavel, P., Sonbawne, S. M., Patil, R. D. and Maheskumar, R. S., 2016, "Investigation of aerosol indirect effects on monsoon clouds using ground-based measurements over a high-altitude site in Western Ghats", *Atmospheric Chemistry and Physics*, **16**, 8423-8430, doi:10.5194/acp-16-8423-2016.

Bonacina, L. C. W., 1945, "Orographic rainfall and it's place in the hydrology of the globe", *Quarterly Journal of Royal Meteorological Society*, **71,** 41-55.

De, U. S. and Dutta S., 2005, "West coast rainfall and convective instability", *Indian journal of Geophysical Union*, **9**, 71-82.

De, U. S., 1973, "Some studies on mountain waves", Ph. D. thesis, Banaras Hindu University, India.

Dee, D. P., Uppala, S. M., Simmons, A. J., Berrisford, P., Poli, P., Kobayashi, S., Andrae, U., Balmaseda, M. A., Balsamo, G., Bauer, P., Bechtold, P., Beljaars, A. C. M., Berg, L. vande, Bidlot, J., Bormann, N., Delsol, C., Dragani, R., Fuentes, M., Geer, A. J., Haimberger, L., Healy, S. B., Hersbach, H., Hólm, E. V., Isaksen, L., Kållberg, P., Köhler, M., Matricardi, M., McNally, A. P., Monge Sanz, B. M., Morcrette, J. J., Park, B. K., Peubey, C., Rosnay, P. de, Tavolato, C., Thépaut, J. N. and Vitart, F., 2011, "The ERA-Interim reanalysis: configuration and performance of the data assimilation system", *Quarterly Journal of RoyalMeteorological Society*, **137,** 553-597 Part A doi: 10.1002/qj.828.

Draxler, R. R. and Rolph, G. D., 2003, "HYSPLIT (HYbrid Single-particle Lagrangian Integrated Trajectory)", NOAA Air Resources Laboratory, Silver Spring, MD Model access via NOAA ARL READY Website.

Dutta, S., 2005, "Effect of static stability on thepattern of three dimensional baroclinic lee wave across a mesoscale elliptical barrier", *Meteorologyand Atmosphric Physics*, **90,** 139-152.

Dutta, S., 2007, "A meso-scale thre-dimensional dynamical model of orographic rainfall", *Meteorologyand Atmospheric Physics*, **95**, 1-14, doi: 10.1007/s00703-006-0195-6.

Dutta, Somenath., Khare, P. and Tathe, A. D., 2015, "Isolated heavy rainfall over sylhet, bangladesh and convective instability", *MAUSAM*, **66**, 4, 675-686.

Grossman, R. L. and Durran, D. R., 1984, "Interaction of low-level flow with the Western-Ghat mountains and off-shore convection in the summer monsoon", *Monthly WeatherReview*, **112**, 652-671.

Indian Daily Weather Report (IDWR), June-September 2015.

Konwar, M., Das, S. K., Deshpande, S. M., Chakravarty, K. and Goswami, B. N., 2014, "Microphysics of clouds and rain over the western Ghats", *Jornal of Geophysical Research Atmosphere*, **119**, 6140-6159.

Krishnamurti, T. N., 1986, "Work book on Numerical weather prediction for tropics for class I and II personnel", WMO technical publication No. **669**, 127-143.

Kumar, Siddharth, Hazra, A. and Goswami, B. N., 2014, "Role of interaction between dynamics, thermodynamics and cloud microphysics on summer monsoon precipitating clouds over the Myanmar Coast and the Western Ghats", *Climate Dynamics*, **43**, 911-924, doi: 10.1007/s00382-013-1909-3.

Leena, P. P., Anilkumar, V., Sravanthi, N., Patil, R., Chakravarty, K., Saha, S. K. and Pandithurai, G., 2018, "On the precipitation susceptibility of monsoon clouds to aerosols using high altitude ground-based observations over Western Ghats, India", *Atmospheric Environmen.*, **185**, 128-136.

Leena, P. P., Pandithurai, G., Anilkumar, V., Murugavel, P., Sonbawne, S. M. and Dani, K. K., 2016, "Seasonal variability in aerosol, CCN and their relationship observed at a high altitude site in Western Ghats", *Meteorology and Atmospheric Physics*, **128,** 143-153, doi: 10.1007/s00703-015-0406-0.

Levin, Z. and Cotton, W., 2008, "Aerosol pollution impact on precipitation : A scientific review", *WMO/IUGG Rep*., p482.

Lowenthal, D. H., Borys, R. D., Choularton, T. W., Bower, K. N., Flynn M. J. and Gallagher, M. W., 2004, "Parameterization of the cloud droplet-sulfate relationship", *Atmospheric Environment*, **38**, 287-292.

Lynn, B., Khain, A., Rosenfeld, D. and Woodley, W. L., 2007, "Effects of aerosols on precipitation from orographic clouds", *Journal of Geophysical Research*, **112**, D10225, doi: 10.1029/2006JD00 7537.

Madan, O. P., Mohanty, U. C., Iyenger, Gopal, Shivhare, R. P., Prasad Rao, A. S. K. A. V., Sam, N. V. and Bhatla, R., 2005, "Off shore trough and very heavy rainfall events along the West Coast of India during ARMEX-2002", *MAUSAM*, **56**, 1, 37-48.

Mahakur, M., Prabhu, A., Sharma, A. K., Rao, V. R., Senroy, S., Singh, Randhir and Goswami, B. N., 2013, "A high-resolution outgoing longwave radiation dataset from Kalpana-1 satellite during 2004-2012", *Current Science*, **105**, 1124-1133.

Maheskumar, R. S., Narkhedkar, S. G., Morwal, S. B., Padmakumari, B., Kothawale, D. R., Joshi, R. R., Deshpande, C. G., Bhalwankar, R. V. and Kulkarni, J. R., 2014, "Mechanism of high rainfall over the India west coast region during the monsoon season", *Climate Dynamics*, **43**, 1513-152, doi :10.1007/s00382-013-1972-9.

Menon, S., Denman, K. L., Brasseur, G., Chidthaisong, A., Ciais, P., Cox, P. M., Dickinson, R. E., Hauglustaine, D., Heinze, C., Holland, E. and Jacob, D., 2007, "Couplings between changes in the climate system and biogeochemistry (No. LBNL-464E)", Lawrence Berkeley National Lab. (LBNL), Berkeley, CA (United States).

Muhlbauer, A. and Lohmann, U., 2009, "Sensitivity Studies of Aerosol-Cloud Interactions in Mixed-Phase Orographic Precipitation", *Journal of Atmospheric Science*, **66,** 2517-2538.

Niyogi, D., Chang, H. I., Chen, F., Gu, L., Kumar, A., Menon, S. and Pielke, R. A. Sr., 2007, "Potential impacts of aerosol-land-atmosphere interactions on the Indian monsoonal rainfall characteristics", *Natural Hazards*, **42**, 345-359. doi: 10.1007/ s11069-006-9085-y.

Peng, Y., Lohmann, U., Leaitch, R., Banic, C. and Couture, M., 2002, "The cloud albedo-cloud dropleteffective radius relationship for clean and polluted clouds from RACE and FIRE", *ACE Journal of Geophysical Research*, **107**, 4106, doi: 10.1029/2000J D000281.

Rotunno, R. and Ferretti, R., 2001, "Mechanisms of intense Alpine rainall", *Journal of Atmospheric Science*, **58**, 1732-1749.

Sarker, R. P., 1966, "A dynamical model of orogaphic rainfall", *Monthly Weather Review*, **94,** 555-572.

Sarker, R. P., 1967, "Some modifications in a dynamical model of orographic rainfall", *Monthly Weather Review*, **95,** 673-684.

Singla, V., Mukherjee, S., Safai, P. D., Meena, G. S., Dani, K. K. and Pandithurai, G., 2017, "Role of organic aerosols in CCN activation and closure over a rural background site in Western Ghats, India", *Atmospheric Environment*, **158**, 148-159.

Twomey, S., Piepgrass, M. and Wolfe, T., 1984, "An assessment of the impact of pollution on global cloud albedo", *Tellus*, **36B**, 356-366.

Utsav, B., Deshpande, S. M., Das, Subrata, K. and Pandithurai G., 2017, "Statistical characteristics of convective clouds over the Western Ghats derived from weather radar observations", *Journal of Geophysical Research*, **122,** 1-27.

Watnabe, H. and Ogura, V., 1987, "Effects of orographically forecd upstream lifting on mesoscale heavy precipitation : A case study", *Journal of Atmospheric Science*, **44,** 661-675.